Early development of a polycaprolactone electrospun augment for anterior cruciate ligament reconstruction

Luka Savić[1], Edyta M Augustyniak[1], Adele Kastensson [1], Sarah Snelling[1], Roxanna E Abhari[1], Mathew Baldwin[1,2], Andrew Price[1,2], William Jackson[2], Andrew Carr[1,2], Pierre-Alexis Mouthuy[1] *

[1] Botnar Institute of Musculoskeletal Sciences, Nuffield Department of Orthopaedics, Rheumatology and Musculoskeletal Sciences, University of Oxford, Oxford, UK

[2] Nuffield Orthopaedic Centre, Oxford University Hospitals NHS Trust, Oxford, UK

*corresponding author: pierre-alexis.mouthuy@ndorms.ox.ac.uk

Keywords: *ACL Reconstruction, Medical textiles, Electrospinning, Polycaprolactone, Tissue Regeneration*

Abstract

Despite the clinical success of Anterior Cruciate Ligament reconstruction (ACLR) in some patients, unsatisfactory clinical outcomes secondary to graft failure are seen, indicating the need to develop new regeneration strategies. The use of degradable and bioactive textiles has the potential to improve the biological repair of soft tissue. Electrospun (ES) filaments are particularly promising as they have the ability to mimic the structure of natural tissues and influence endogenous cell behaviour. In this study, we produced continuous polycaprolactone (PCL) ES filaments using a previously described electrospinning collection method. These filaments were stretched, twisted, and assembled into woven structures. The morphological, tensile, and biological properties of the woven fabric were then assessed. Scanning electron microscopy (SEM) images highlighted the aligned and ACL-like microfibre structure found in the stretched filaments. The tensile properties indicated that the ES fabric reached suitable strengths for a use as an ACLR augmentation device. Human ACL-derived cell cultured on the fabric showed approximately a 3-fold increase in cell number over 2 weeks and this was equivalent to a collagen coated synthetic suture commonly used in ACLR. Cells generally adopted a more elongated cell morphology on the ES fabric compared to the control suture, aligning themselves in the direction of the microfibres. A NRU assay confirmed that the ES fabric was non-cytotoxic according to regulatory standards. Overall, this study supports the development of ES textiles as augmentation devices for ACLR.

Introduction

The anterior cruciate ligament (ACL) provides mechanical rotational stability to the knee but it can be injured following twisting injuries to the joint. While commonly occurring in young, active individuals, these injuries can lead to significant long-term complications, reducing both quality of life and physical activity. In the United States, it is reported that around 200,000 ruptures occur annually, with up to 100,000 surgical repairs per year (1, 2). In the United Kingdom, surgical intervention of ACL injuries is preferred over conservative management, with up to 80% of patients undergoing surgery, and it is frequently performed for a young active cohort of patients (3, 4). It was estimated that this represents a minimum of 15,000 operations each year, with an associated cost to the NHS of approximately £63 million (4). Globally, the gold standard surgical operation involves an ACL reconstruction (ACLR) using an autologous hamstring or patellar tendon in combination with bony fixation devices (5, 6). In many cases this reconstruction strategy is successful, but donor site morbidity can occur and failure of the ACLR have been reported in between 6 to 31% of cases (7). As a result recurrent knee instability is a major issue that can be observed in the years following surgery. In the longer term, individuals who have undergone ACLR show increased susceptibility to developing knee osteoarthritis (OA) (6, 8-11).

Replacing or augmenting autologous tissue with artificial grafts or ligament devices has been proposed as a strategy in ACLR for more than 40 years. The majority of devices explored to date are made of non-degradable synthetic polymers such as nylon (12), polyethylene terephthalate (13) and polyester (14). While these materials are typically strong and easy to process during implant manufacturing, they often suffer from long-term problems of device

rejection and chronic tissue inflammation due to particle formation (12, 15, 16). They also suffer from short-term issues such as permanent elongation eventually leading to failure (17). Despite these complications, synthetic suture-tape materials designed for ACLR augmentation, such as LabralTape, have gained interest as a result of the biomechanical superiority seen in some studies compared to ACLR alone (18). Ultimately, an increasing focus is to improve the biological repair of ACL tears during augmentation, using biocompatible materials, while maintaining suitable mechanical support. In this context, devices made of biological materials, such as collagen, have been proposed to act as a scaffold for biological repair (19, 20). However, the success of these materials has been limited, mainly due to the poor mechanical properties and concerns related to their immunogenicity (21, 22). Using degradable synthetic polymers can mitigate some of these issues, especially when they are processed through electrospinning (23, 24).

Electrospinning can create fibrous materials that closely mimic the architecture of native extracellular matrix of soft tissues such as tendon and ligaments. This has been shown to be effective at directing cellular behaviour, including proliferation, migration and differentiation (25-27). Our group has previously developed a method to produce continuous filament made of poly(*p*-dioxanone) (PDO), a polymer used in FDA-approved devices which typically degrades fully within 6 months (28-32). These filaments were able to undergo post-spinning processing with industrial textile machinery to design various medical textiles for soft tissue repair. While applied to PDO, this method could be extended to other polymers. Poly(ε-caprolactone) (PCL) is particularly attractive for ACL applications, where higher strengths and slower degradation

(between 2 to 4 years) might be needed (24, 27, 33). Similar to PDO, PCL is a widely used polymer in the field of biomaterials with clear evidence of biocompatibility in human (34-37).

The aim of this study was to demonstrate that our existing method of filament production could be used to create continuous PCL electrospun (ES) filaments and that these could be assembled into a robust fabric that may be suitable for ACLR augmentation. The physical properties of the prototyped scaffolds and its constituents were assessed through tensile testing and scanning electron microscopy (SEM). Moreover, their biocompatibility was investigated using human primary tenocytes cultured on their surface for up to 14 days and using a cytotoxicity assay guided by regulatory standards.

Materials and methods

Preparation of the electrospinning solution

The electrospinning solution was prepared by dissolving PCL (Ashland Specialities Ireland, Laboratory A, Synergy Centre, Institute of Technology Tallaght, Ireland) into 1,1,1,3,3,3-hexafluoroisopropanol (HFIP, Apollo Scientific Ltd, Cheshire, UK) at a concentration of 16% (w/v). The solution was agitated at room temperature on a roller set on speed of 15 RPM for at least 24 h to allow for complete dissolution of the polymer.

Electrospinning continuous PCL filaments

The continuous ES filaments were produced from the polymer solution as described previously (27). Briefly, electrospinning was performed with a single nozzle electrospinning setup and a wire collector (100 μm in diameter, Goodfellow, Huntingdon, UK) using a high voltage power supply system (30 kV, SL30P30/230, Spellman, West Sussex, UK) and a syringe pump (World Precision Instruments Limited, Florida, US). The nozzle and the wire collector were positioned in a glove box under constant airflow to remove organic vapour produced during operation. The wire was cleaned with 70% ethanol prior use. The distance between the nozzle and the wire was 20 cm and the average voltage applied was 8.6 kV. The speed of the wire travelling between the feeding unit and the winding unit was set at 0.5 mm s^{-1}. Following the exit of the metal wire (coated with the PCL material) from the glove box, the ES fibrous mesh was detached as a continuous filament and placed on a separate spool. The filament spool was removed at the end of the process and stored in a desiccator prior to stretching.

Stretching of the raw filament

The filament obtained from the electrospinning step was stretched (drawn) to avoid permanent deformation during further use and reach an elastic behaviour (30). This stretching was performed manually in a clean environment at a ratio of about 1:7. Where brakes occurred, knots were applied to maintain the continuity of the filament. The resulting stretched filament was placed on a new spool and stored in a desiccator prior to twisting.

Twisting filaments into yarns

Stretched filaments were used to produce twisted yarns. The twisting machine (Marui textile machine co., Ltd., Osaka, Japan) worked in combination with an in-house made feeder stand hosting up to 9 spools. Three filaments were twisted in S direction with a spindle speed of 600 to obtain plied yarns. Three plied yarns were then twisted together in the Z direction at a speed of 600 to obtain cabled yarns. The cabled yarns were stored in the desiccator prior to weaving.

Weaving the yarns into fabrics

The cabled yarns were woven manually with weaving loom (Ashford wheels & looms, Ashburton, UK) into a plain weave fabric with a targeted width of 10 mm. To achieve this, 20 cabled yarns were used as the warps and 1 cabled yarn was used as the weft. Control samples for cell culture were prepared by weaving FiberWire® (FW) sutures (Arthrex, US). To achieve a similar design, 20 sutures were used as the warps and 1 suture as the weft. The final woven fabrics were stored in the desiccator prior to further use.

Tensile tests

The samples (ES filaments, yarns, woven fabrics and control sutures) were mechanically characterized using a Zwick tensile machine (Zwick Roell Group, Ulm, Germany). The tests were carried out at the rate of 25 mm/min until failure for all tests (n = 10 for ES samples, n = 4 for FW sutures). The length of the samples was set to 100 mm for the yarn and 50 mm for the fabrics and FW sutures. The force at break (N) and rate of elongation (mm) were recorded. The TestXpert software was used to collect data. All yarn diameters were measured with an electronic digital calliper (Titan, Renton, US). The porosity values of the ES materials were estimated with a weight approach (known length and diameter) and the known density of PCL ($1.145 g/cm^3$). The porosity of FW was set at 27%, based on the known porosity of a similar suture (32).

ACL material, donor demographics and clinical data

ACL tissue was obtained from the Oxford Musculoskeletal Biobank, with informed donor consent in full compliance with the National and Institutional ethical requirements, the United Kingdom Human Tissue Act. Ruptured ACL samples were collected from patients during surgery and transferred immediately into a sterile tube containing DMEM F12 (Lonza, UK) for explanation. ACL-derived cells from each donor were used individually.

ACL-derived cells isolation and culture

ACL samples obtained from the donors were cut into small uniform pieces under sterile conditions and transferred to six well plates (Corning, US) supplemented with growth medium. Growth medium used was Dulbecco's Modified Eagle Medium (DMEM, Sigma-Aldrich, UK) F12 containing 50% foetal bovine serum (FBS, InvitrogenTM, UK) and 1% penicillin–

streptomycin (InvitrogenTM, UK). Plates were incubated at standard conditions (37°C, 5% CO_2) and growth medium was replaced every third day. Once cells had migrated from the explants, after approximately 7 days, the medium was refreshed with DMEM F12 containing 10% FBS. Once cells had reached approximately 90% confluency, they were mechanically scraped and sub-cultured under the same conditions in 10 cm Petri dishes (Greiner, Germany) to allow proliferation. Cells were regularly checked for Mycoplasma infection using a MycoAlert testing kit (Lonza, UK), according to the manufacturer's instructions. ACL derived cells were used in the third passage for consistency and to avoid phenotypic drift.

Cell Seeding

Fabric samples (ES and controls) were cut to 0.5 cm^2 in size and placed in 48 well plates (Corning, UK). All materials were sterilized using 70% ethanol and dried overnight under sterile conditions at RT. Before seeding, cells were counted using a hemocytometer counting-chamber device. ACL-derived cells were then seeded at high density (5×10^4 in 20 µL of cell suspension per scaffold) and subsequently, the scaffolds were placed in a 5% CO_2, 37°C for 2h to allow cells to attach. Then, scaffolds were transferred to a fresh 48-well plate containing 400 µL of DMEM/F-12 media to exclude cells attached to the polystyrene wells of the original plate.

Cell Attachment and Proliferation – PrestoBlue Cell Viability Assay

To assess cell attachment and growth on the samples, a PrestoBlue (Invitrogen, Paisley, UK) assay was used. At selected time points, culture media was aspirated from each well and replaced with 200 µL of 10% PrestoBlue solution (v/v in DMEM/F-12). After 1 hour of incubation at 37°C, 100 µL of PrestoBlue medium samples from each well were transferred to a black 96-well

plates (Corning, UK) for analysis. Fluorescence was measured using the FluoStar Optima microplate reader (BMG Labtech, Ortenberg, Germany, λ_{ex} = 544 nm, λ_{em} = 590 nm). The remaining PrestoBlue medium was removed and replaced with a fresh standard medium. The experiments were performed with three different patients (n = 3), each in minimum of triplicates.

Maintenance of BALB/c 3T3 Cells

BALB/c 3T3 cells (Merck, Germany) were maintained at 37°C in 5% CO_2 in Dulbecco's Modified Eagle Medium (DMEM, Sigma-Aldrich, UK) supplemented with 10% (v/v) newborn calf serum (Sigma-Aldrich, UK), 4 mM L-glutamine (Thermo Fisher Scientific, UK), 20 mM HEPES (Thermo Fisher Scientific, UK), and 1% (v/v) penicillin/streptomycin (InvitrogenTM, UK). Cells were cultured in 10 cm Petri dishes (Greiner Bio-One, UK). The culture media was changed every third day. Once cells had reached approximately 90% confluency, they were mechanically scraped and sub-cultured under the same conditions in 10 cm Petri dishes (Greiner, Germany) to allow proliferation. Cells were regularly checked for Mycoplasma infection using a MycoAlert testing kit (Lonza, UK), according to the manufacturer's instructions.

NRU Cytotoxicity Assay

For the Neutral red uptake (NRU) cytotoxicity test, BALB/c 3T3 cells which were seeded into 96-well plates (1 x 10^4 cells/well) and maintained in culture for 24 h (approximately 1 doubling period) to form a sub-confluent monolayer. Subsequently, cells were exposed to the test compounds over a range of concentrations. After 24 h exposure, NRU was determined for each treatment concentration and compared to that determined in control cultures – cell viability was calculated as the percentage of vehicle control (cell culture media only) values. For the treatment

extracts, all compounds were extracted at a ratio of 0.1 mg/ml in vehicle medium for 72 h before being added to cell culture.

Scanning Electron Microscopy

Scaffolds with cells were fixed in 2.5% v/v glutaraldehyde in deionised water for 1 hour at room temperature. The fixative was removed and the samples were rinsed trice in PBS before undergoing sequential dehydration in a graded ethanol series (40%, 50%, 70%, 90%, and 2 x 100% ethanol v/v in MiliQ H_2O, 10 minutes each step). Scaffolds were further dehydrated using hexamethyldisilazane (HMDS, 300 µL/scaffold) and were left inside the fume cupboard overnight to complete drying. Samples were stored in a desiccator until use. Before imaging, scaffolds were mounted on an aluminium stub using a carbon adhesive disk and gold-coated using a sputter coater (SC7620 mini, Quantum Design, Switzerland). High-resolution images were taken using an environmental scanning electron microscope (Evo LS15 Variable Pressure Scanning Electron Microscope, Carl Zeiss, Germany). Multiple areas (minimum of 3) were observed randomly on each sample at magnifications of ×100, ×500, ×1000, and ×5000. The microfibre diameter was measured based on images taken at ×5000 magnification using Image J (38). A total of 10 measurements were performed for type of sample.

Statistical analysis

The statistical analysis was performed with the GraphPad Prism software version 8 (GraphPad Software, San Diego, USA). Data in graphs were expressed as means with standard deviations. T-tests and standard ANOVA with Tukey's multiple comparisons testing were used to examine statistical differences between groups. Results were considered significant for $p < 0.05$.

Results

Manufacturing stretched PCL ES filaments

Continuous PCL ES filaments were successfully produced with the wire collector system, as shown in Figure 1. The collected or 'raw' filaments presented as flat meshes of randomly arranged of microfibres (Figure 1A and B). These were drawn to obtain stretched filaments made of aligned microfibres (Figure 1C-E). Besides alignment, stretching also resulted in reducing the average width of the filaments from 776 to 517 μm and in decreasing the average microfibre diameter from 2.9 ± 0.6 μm to 1.9 ± 0.4 μm (Table 1). A representative curve shown in Figure 1 F indicates that stretched filaments have a near linear stress-strain behaviour under tension.

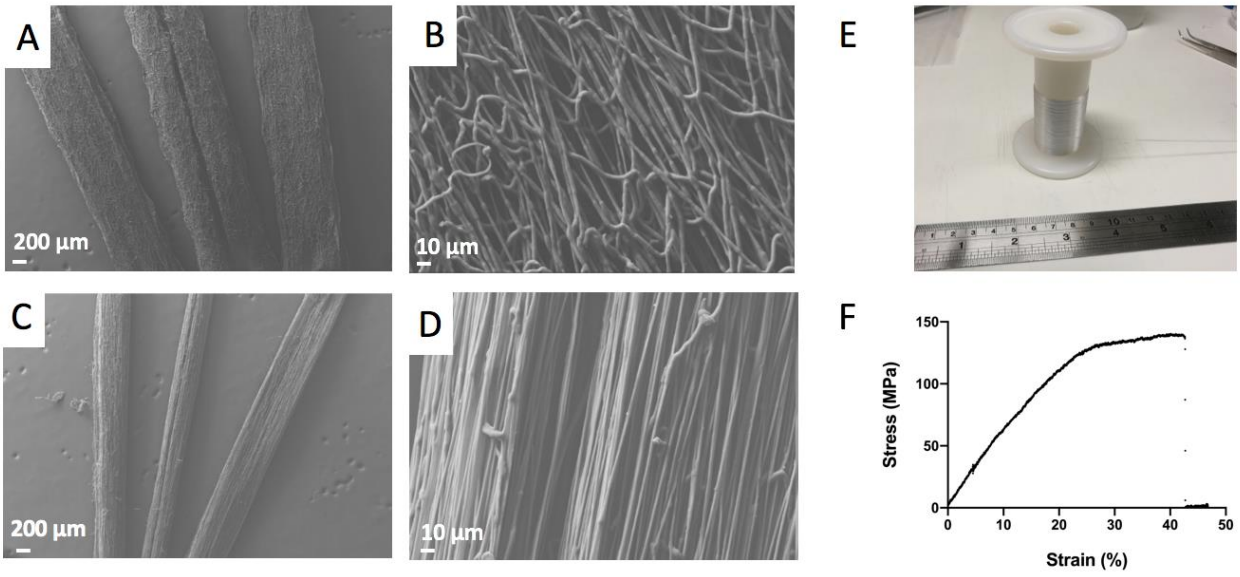

Figure 1: Producing stretched PCL ES filaments: A-B. SEM images of collected, unstretched, filaments (400x and 2500x, respectively) showing a relatively random microfibre arrangement, C-D. SEM images of stretched filaments at similar magnification, showing a smaller width and aligned microfiber arrangement, E.

macroscopic image of a spool of stretched filament, D. Typical stress-strain curve obtained during tensile test to failure showing the elastic behaviour of a stretched filament.

Assembling multifilament twisted yarns

Plied yarns (made of 3 stretched filaments) and cabled yarns (made of 3 plied yarns) were both produced with an automated twister, as shown in Figure 2. As shown in Table 1, similar twist numbers were measured in the plied yarns and cabled yarns: 184 ± 44 twists/m (S direction) and 172 ± 33 twists/m (Z direction), respectively. The average diameter of the microfibres in the stretched filaments was shown to decrease further to 1.6 ± 0.4 µm in the cabled yarns.

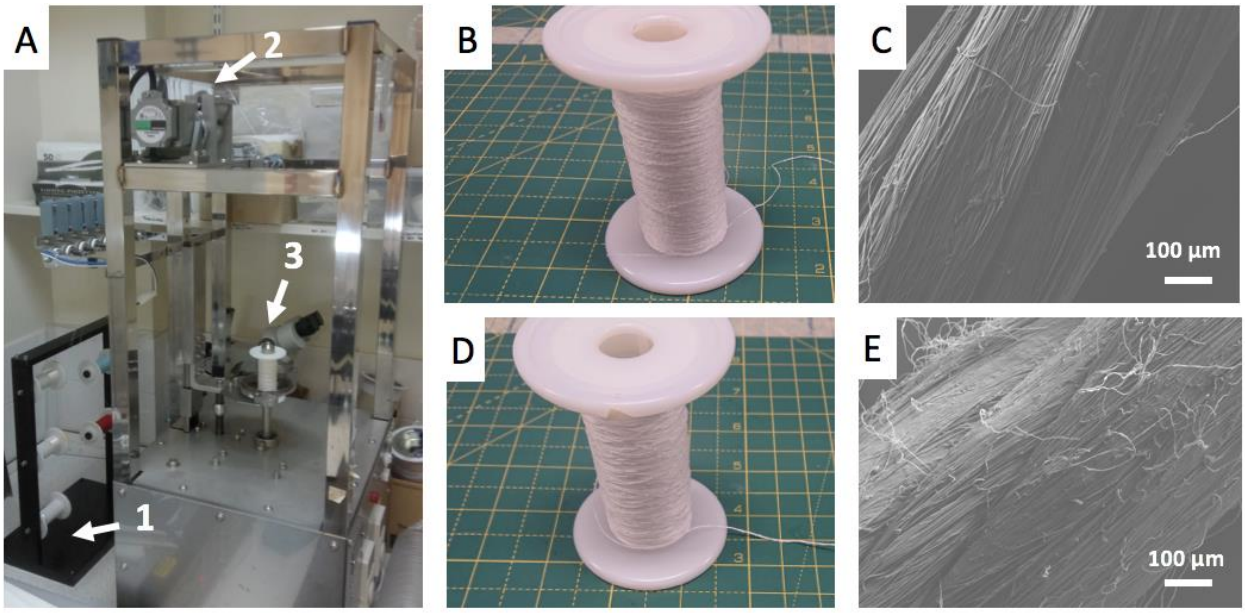

Figure 2: Assembling multifilament yarns: A. Macroscopic picture of the automated twisting unit used to produce the yarns (1: feeding stand; 2: feeding motor, 3: collecting spool), B. Spool of plied yarn, C. SEM image of a plied yarn, D. Spool of cabled yarn, E. SEM image of a cabled yarn.

The tensile tests showed that the force at break progressively increased from 2.0 ± 0.4 N, 5.8 ± 0.5 N, and 14.8 ± 0.8 N for the stretched filament, plied yarn and cable yarn, respectively (Figure 3A). The maximum stress changed from 152.0 ± 33.4 MPa, 191.0 ± 15.7 MPa, 144.2 ± 7.7 MPa with the increase in hierarchical structure (Figure 3B). The maximum elongation was around 40-50% for all structures, with no significant difference between samples (Figure 3C). The Young's modulus followed a trend similar to the maximum stress, showing 536.4 ± 82.9 MPa, 657.3 ± 76.4 MPa, 418.8 ± 23.3 MPa, respectively for the filament, plied yarn and cabled yarn (Figure 3D).

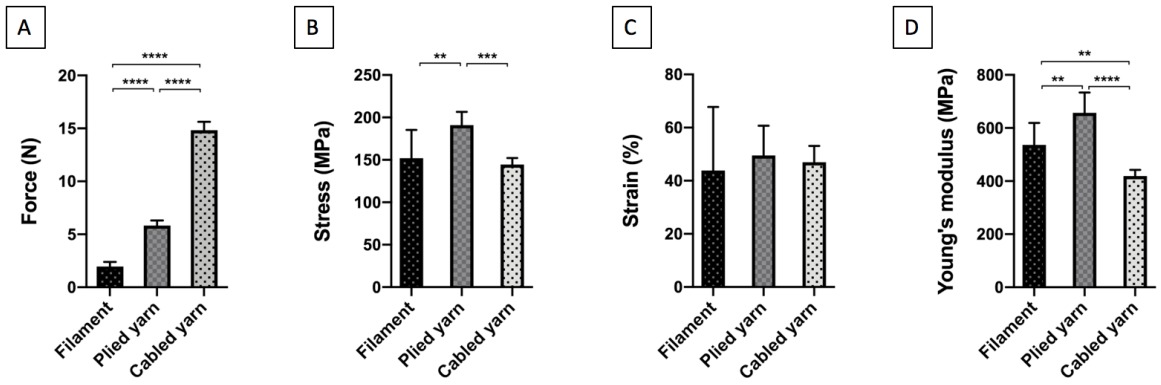

Figure 3: Tensile properties of the stretched filament, plied yarn and cabled yarn: A. maximum force, B. maximum stress, C. strain at maximum stress, and D. Young's modulus. Error bars represent standard deviation (n=10), ****p<0.0001 *** p<0.001 **p<0.01.

Table 1: Textile properties of the PCL ES filaments and yarns (N/A: not applicable)

	Diameter or width (μm)	Microfiber diameter (μm)	Twist number (twists/m)	Linear density (dTex)	Fibre tenacity (cN/dtex)
Unstretched filament	776.1 ± 229.1	2.9 ± 0.6	N/A	-	-
Stretched filament	516.5 ± 93.6	1.9 ± 0.4	N/A	145.2 ± 13.6	1.4 ± 0.3
Plied yarn	433.4 ± 73.3	1.9 ± 0.3	184 ± 44	343.0 ± 12.8	1.7 ± 0.2
Cabled yarn	580.0 ± 51.6	1.6 ± 0.	172 ± 33	1136.8 ± 40.4	1.3 ± 0.1

Weaving the ES fabric

As shown in Figure 4 A-C, a 10 mm-wide plain pattern fabric was produced with a manual loom. The fabric was made of 20 cabled yarns as the warps (yarns travelling in the direction of the fabric) and 1 cabled yarn used as the weft (yarn travelling side-to-side). Approximately 2 meters of fabric were produced in this study, corresponding to about 1 km of stretched filament.

The mechanical properties of the ES fabric are shown in Figure 4 D-G and are compared to FibreWire (FW) sutures. The maximum force measured for the ES fabric was 272.6 ± 13.5 N. This was inferior to the force measured for FW sutures, which was 326.4 ± 11.1 N. However, all the ES samples failed at the grips, indicating that clamping may have damaged the fabric and

that higher forces could be reached with more suitable grips. The maximum strain was measured to be or 75 ± 7% and 36 ± 13%, respectively for the ES fabric and the FW suture. The maximum stress was much lower for the ES fabric, 70.0 ± 3.5 MPa, than for the control, 319.0 ± 12.5 MPa. Similarly, the Young modulus was 116.1 ± 9.3 MPa and 1441 ± 414 MPa, respectively. This indicates that the suture is stronger and much stiffer than the ES fabric.

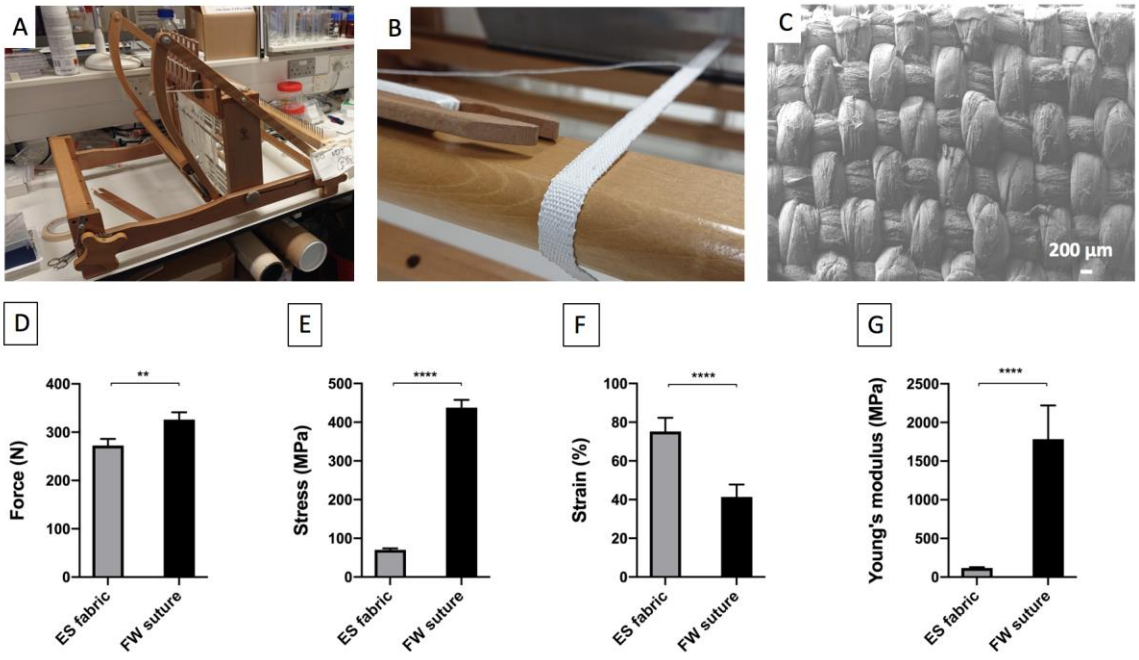

Figure 4: Woven ES fabric produced from ES cabled yarns: A. manual weaving loom used in this study; B woven band under production showing a plain weave pattern; C. SEM image of woven fabric size at low magnification; D-G. Mechanical data comparing the woven PCL fabric to FW sutures (control) including maximum force (D), maximum stress (E), strain at maximum stress (F) and Young's modulus (G). **** $p<0.0001$ ** $p<0.01$.

Biological characterisation with primary human ACL-derived cells

The attachment, proliferation and morphology of primary human ACL-derived cells on the ES fabric are shown in Figure 5. The initial cell attachment was not significantly different between the ES fabric and the FW control (Figure 5A). Only a small proportion of the cells seeded attached to either substrates, as shown by the low seeding efficiency of around 25% in Figure 5B. However, cells proliferated over 14 days, and showed a similar growth curve for both types of materials (Figure 5C). On day 4, cells on the ES fabric aligned with the fibre direction (Figure 5D). Cell alignment was less pronounced on the FW control, as cells tended to wrap around the larger fibres and bridge bigger fibre gaps (Figure 5G). Higher coverage of the materials by cells can be seen at day 7 (Figures 5E-H). At day 14, there was a significant increase in biomass relative to day 1 (Figure 5C, $p > 0.05$) for both substrates, with cells almost fully covering their surfaces (Figures 5F and I).

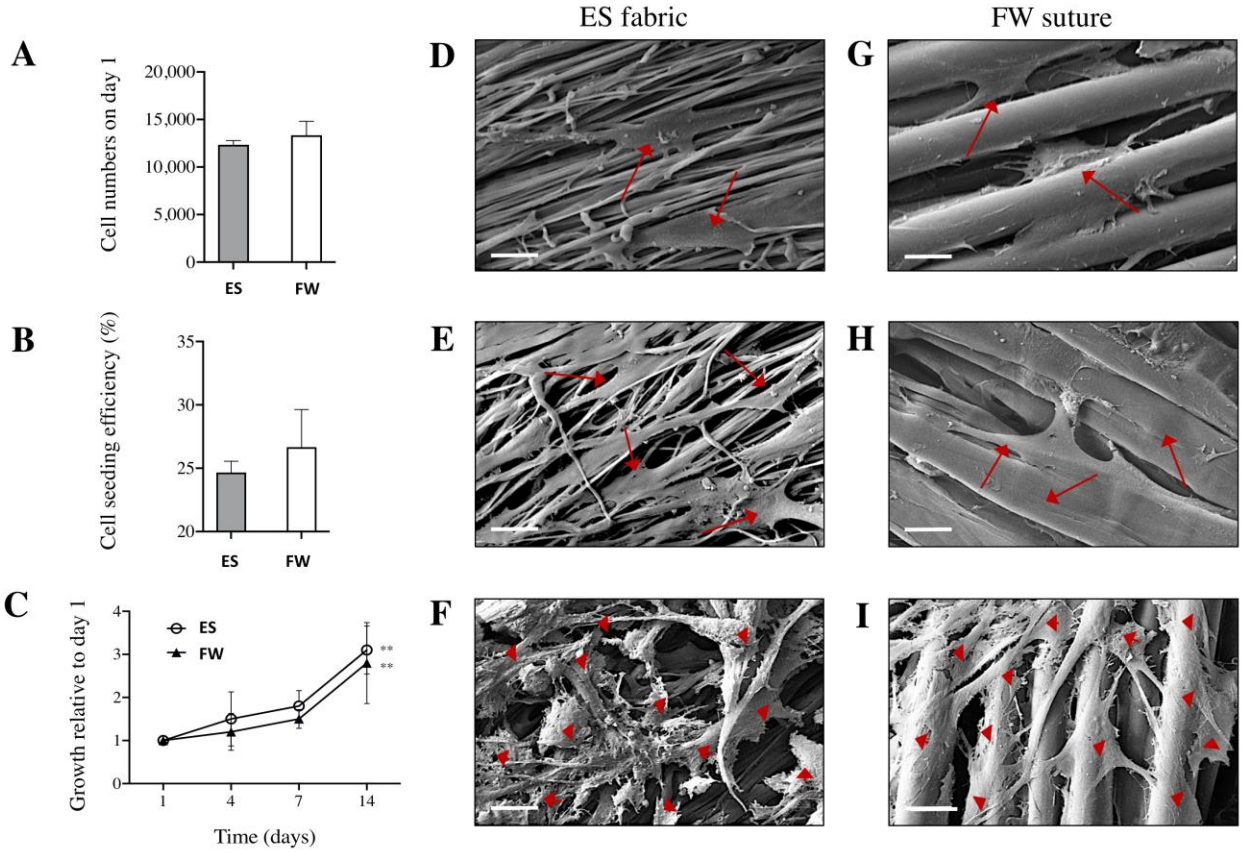

Figure 5. *In vitro* comparison of the ES fabric and FW sutures using a primary human ACL-derived model. A. Numbers of cells attached to the materials 24 hours after seeding. B. Cell seeding efficiency. C. Relative cell growth on the materials over 14 days (Mean ± SD, Two-way ANOVA with Tukey's post hoc test; n = 3, each in min. of triplicates; ** $p < 0.05$). D – F. SEM images showing cell morphology and spreading on the ES fabric (red arrows) at day 4 (D), day 7 (E), and day 14 (F) after seeding. G – I. SEM images showing cell morphology and spreading on FW (red arrows) at day 4 (G), day 7 (H), and day 14 (I). Scale bars = 20 μm

Cytotoxicity of the ES fabric

The NRU assay – an indirect cytoxicity test recommended as part of the biological evaluation of medical devices – is based on the ability of viable cells to incorporate and bind the supravital dye neutral red in lysosomes, thus providing a semi-quantitative estimation of the number of viable cells in a cell culture. Here, we have used an in-house NRU assay for preliminary assessment of the biocompatibility of an ES fabric as guided by the ISO 10993-5:2009 standard. The 3T3 mouse fibroblast cell line was exposed to test compounds over a range of concentrations (Figure 6A). After 24 h exposure, NRU was determined for each treatment concentration and compared to that of control culture. The results of the indirect cytotoxicity test confirmed ES fabric is non-cytotoxic, with relative cell viability for the highest concentration of the sample extract (neat extract) being ≥ 70 % of the control group – a minimum required by ISO-10993-5 to pass this test. Figure 6B shows SLS control testing within the specified range, a test acceptability criterion.

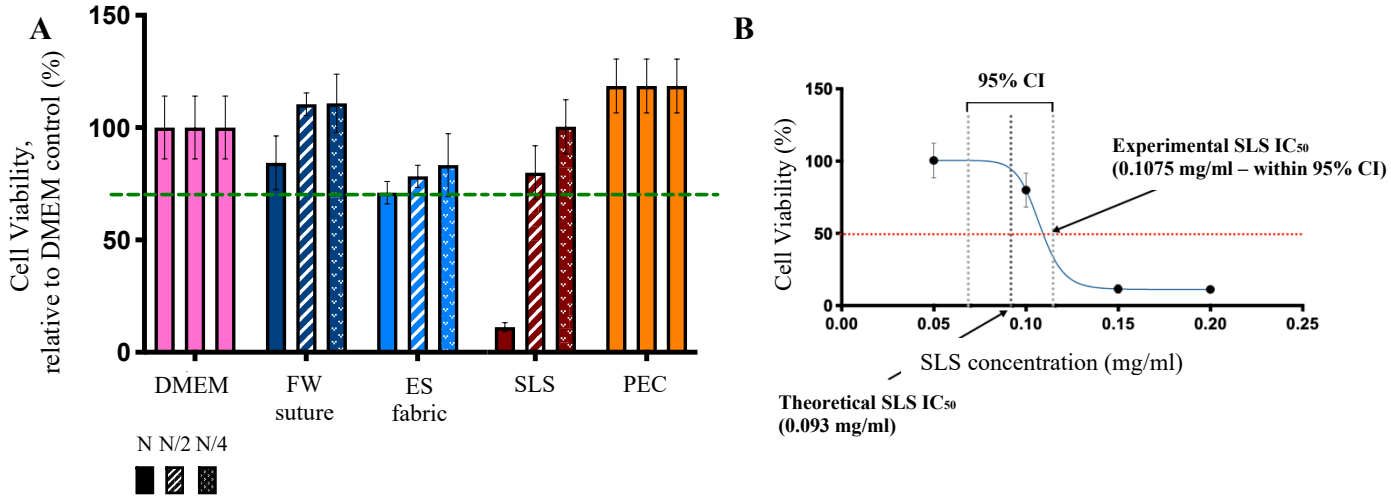

Figure 6. Cytotoxicity of the ES fabric as determined by the NRU test. A. Comparison of cytotoxicity of FW suture (dark blue) and ES fabric (light blue) groups test compounds over a range of concentrations. N represents undiluted extract. N/2 and N/4 represent 2-fold and 4-fold dilutions of N, respectively. DMEM represents media only (vehicle) control group; SLS (sodium dodecyl sulphate) represent positive control group; PEC (polyethylene caps) represents negative control group. B. SLS. Intra- and interlaboratory repeat test control.

Discussion

Bioactive and degradable (or resorbable) synthetic textiles that encourage tissue repair are a promising strategy to biologically and mechanically support ACL reconstruction or repair (21, 39-41). While the mechanical properties of those textiles are important to sustain the significant stresses at the ACL reconstruction site, physical cues at the microlevel are also key to instruct the cells to form new tissue before the material is completely absorbed by the body. Mimicking the alignment and dimensions of the extracellular matrix (ECM) components through processing method such as electrospinning seems to be particularly promising (23, 25, 41, 42). In this context, the ability to produce continuous ES filaments is a key advantage as it enables the production of various fibrous devices using existing textile machineries (29).

Here, we demonstrate that continuous PCL filaments can be produced with an electrospinning method previously proposed for fabricating PDO filaments. This suggests that the wire collection method is not polymer specific and could be extended to a wider range of polymers used in the biomaterial field such as polylactic acid, poly(lactic-co-glycolic acid), poly(hydroxy butyrate), *etc*. Moreover, similar to our studies performed with PDO (27), the collected PCL ES filaments could be permanently deformed through stretching to create highly aligned microfibrous structure closely resembling the ECM of ligaments and to reach a near linear elastic behaviour (Figure 1F). The plastic deformation resulting from the stretching also led to a decrease of both the filament width and the microfiber diameter, as previously observed (30). Interestingly, the stretched filaments showed higher values of maximum stress and Young modulus compared to other PCL yarns proposed in the literature. The values measured here were around 150MPa for

the stress and 500MPa for the modulus, while these are typically reported to be between 3-40MPa and 5-70MPa, respectively (43-45). The differences may be explained by the use of the wire collector, as the small surface area available for collection creates a rounded, densely interconnected mesh of fibres. This was shown to improve the strength and stiffness of the yarns compared to 2D collectors (27). The addition of a stretching step post-spinning may also have contributed to this through alignment of the polymer chains along the length of the fibres (46).

Processing the ES filaments into a ES fabric led to a progressive decrease of the average diameter of the microfibres (from 2.9 μm in the single stretched filaments to 1.9 μm in the plied and cabled yarn, and 1.6 μm in the woven fabric). This could be explained by further plastic deformation occurring in the filaments, due to torsion and tension forces caused by the twisting and winding processes. The effect from external forces on deformation is well-known in the production and post-processing of polymeric fibres (47).

The maximum strength of the yarns increased almost linearly with the number of filaments, as expected. The fact that cabled yarns were weaker than anticipated (14.8 N instead of 18 N, *i.e.* 9 x 2 N) may be due to damage caused during the twisting process or to uneven tensions in the final multifilament yarns (47). The maximum strain was also affected when going from single filament to multifilament but it did not vary significantly between plied and cabled yarns. Values of the maximum stress and Young modulus both increased in the plied yarn but dropped in the cabled yarn. Such observations may be the result of the introduction of a high twist number in the plied yarn, resulting in a structure under high tension. This tension was then reduced in the cabled yarns, following twisting in the opposite direction. It is worth noting that, although

418 twisted and woven ES yarns have been proposed before (27, 48-52), post-spinning processing
419 pure ES filaments with an automated twisting unit and with a traditional manual loom are both
420 shown here for the first time. This further supports our previous observations that continuous ES
421 filaments produced with the wire collection system can be processed through a wide range of
422 existing textile technologies (27, 29, 30, 32). This also demonstrates the potential of scaling-up
423 the manufacturing process of PCL ES fabrics.
424
425
426 Weaving the multifilament yarns was necessary to provide the device with dimensions and
427 strength suitable for a potential augmentation role in ACLR. The strength to failure of the woven
428 ES structure was 272.6N, which was near to the expected strength of 20 warps (296 N). In
429 healthy adults the ultimate strength of the native ACL is approximately 2000 N (53) and peak
430 ACL tensile forces during non-weight bearing and weight bearing exercises mostly vary between
431 0 and 400N (16, 54). However, such strength would not be required for an augmentation role in
432 ALCR surgeries, as the materials would be used alongside with an autograft or allograft. FW
433 sutures, which are commonly used in such operations, display an average maximum force of
434 326.4 N. A force at break of 272.6N (*i.e.* about 83% of FW) therefore suggests ES fabrics may
435 be suitable as an augmentation material. To our knowledge this is the first time that pure PCL
436 electrospun fabrics demonstrate such high strengths. However, future work should demonstrate
437 the compatibility of the material with fixation devices (screws and suspensory fixation loops),
438 since these may weaken or damage the soft PCL fabric (as observed in our tensile test at the grip
439 site). Another aspect that requires further work is the design or pattern of the fabric, as here we
440 have been working with a basic plain pattern. Advanced patterns (such as twill) or textile
441 techniques (such as braiding) offer the potential for modulating the mechanical properties

(especially strain and Young modulus but also resistance to fraying), such as to better match those of the native tissue or improve the biological response (32, 55). It is worth noting that, upon implantation, new tissue formation and material degradation would both contribute to the mechanical properties of the device.

Human cells derived from ACL tissue attached and proliferated similarly on both on the ES fabric and the collagen coated FW control. The relatively low seeding efficiency may be explained by the small size of the ES and FW samples and the gaps between fibres in the woven structures, which resulted in most of the cell suspension flowing down to the bottom of the well-plate. While FW (coated and uncoated) has been reported to demonstrate excellent biocompatibility through extensive animal and clinical testing as well as successful clinical outcomes in millions of orthopaedic procedures (56), these results cannot simply be translated into clinical equivalence. However, they are a useful foundation for future preclinical and clinical non-inferiority evaluations.

A difference could be seen in terms of cell morphology as the ES fabric was better at directing and supporting cell alignment compared to FW. These observations are consistent with the literature and is an expected cell response to the highly aligned microfibers present in the ES fabric (57). While these results are encouraging, future work demonstrating cell migration within the materials and looking at their gene expression profile will be important to discuss the healing potential of the ES fabric (27, 29, 58-60).

To complement our biological evaluation, we have carried out a NRU assay guided by the ISO 10993-5:2009 standard. Our results suggest that the proposed PCL ES fabric is not cytotoxic. While the excellent biocompatibility and safety profile of PCL is well-documented, the manufacturing processes carried out to transform PCL into useful medical devices may affect their cytotoxicity. In particular, residual solvents can be the cause of toxicity in electrospun materials as electrospinning often requires the use of organic solvents (*e.g.* HFIP in this case). The results are therefore supportive, although they will need to be repeated at later stages of the product development such as to encompass the effect of sterilisation. It is worth noting that sterilisation is likely to impact various properties of the implant, not just cytotoxicity (61-63).

Overall, our physical and biological evaluations suggest that PCL ES fabrics could act as suitable augmentation devices for ACLR surgeries. The main advantages of PCL ES devices are that they are (1) synthetic, ensuring consistent manufacturing, (2) fully degradable, avoiding problems of long-term rejection, and (3) porous structures made of aligned microfibers, which encourage cell proliferation and fibroblast like morphology. From a regulatory point of view, ES fabrics would classify as a medical device Class III (64). This means that their translation to clinical use and market will require a much more comprehensive set of preclinical tests, including (but not limited to): residual study, chemical analysis, bioburden test, degradation profile and further *in vitro* and *in vivo* (systemic and local toxicity) testing.

Conclusions

Synthetic degradable materials that both support ACLR mechanically and biologically are much sought after. In this context, we have investigated the potential of a fabric made of PCL ES filaments. We used continuous textile processes to create an ES fabric with strengths that could be suitable for an augmentation role in ACLR. Cell proliferation showed approximately a 3-fold increase in cell number over 2 weeks and was equivalent to a collagen coated synthetic suture commonly used in ACLR. The cells generally adopted a better fibroblast morphology on the ES fabric, aligning themselves in the direction of the microfibres. We also demonstrated that the current version of the ES fabric was non-cytotoxic according to established regulatory standards. Overall, this study supports the potential of ES medical textiles for ACLR. Future work will aim at further developing the device such as through the use of braiding, with clinically relevant mechanical testing, degradation assays and more advanced biological testing.

Acknowledgments

This research was funded by the NIHR Oxford Biomedical Research Centre, the Norman Collisson Foundation (NCF) and Versus Arthritis (VA). The views expressed are those of the authors and not necessarily those of the NIHR, the NCF or VA. We also acknowledge the support of the UKRMP smart material hub and the author LS was partially supported through the H2020 Erasmus+ programme. The authors acknowledge the assistance of the IBME workshop, in particular Mr James Fisk and Mr David Salisbury. We also thank Prof Maja Somogyi Škoc for

providing mentorship to LS during the H2020 Erasmus+ project and Dr Kalin Dragnevski for his support with electron microscopy.

References

1. Spindler KP, Wright RW. Anterior Cruciate Ligament Tear. New England Journal of Medicine. 2008;359(20):2135-42.
2. Montalvo AM, Schneider DK, Yut L, Webster KE, Beynnon B, Kocher MS, et al. "What's my risk of sustaining an ACL injury while playing sports?" A systematic review with meta-analysis. Br J Sports Med. 2019;53(16):1003-12.
3. Jameson SS, Dowen D, James P, Serrano-Pedraza I, Reed MR, Deehan D. Complications following anterior cruciate ligament reconstruction in the English NHS. The Knee. 2012;19(1):14-9.
4. Davies L, Cook J, Leal J, Areia CM, Shirkey B, Jackson W, et al. Comparison of the clinical and cost effectiveness of two management strategies (rehabilitation versus surgical reconstruction) for non-acute anterior cruciate ligament (ACL) injury: study protocol for the ACL SNNAP randomised controlled trial. Trials. 2020;21(1):405.
5. Paterno MV. Incidence and Predictors of Second Anterior Cruciate Ligament Injury After Primary Reconstruction and Return to Sport. J Athl Train. 2015;50(10):1097-9.
6. Vaishya R, Agarwal A, ingole s, Vijay V. Current Trends in Anterior Cruciate Ligament Reconstruction: A Review. Cureus. 2015;7:e378.
7. Kartus J, Movin T, Karlsson J. Donor-site morbidity and anterior knee problems after anterior cruciate ligament reconstruction using autografts. Arthroscopy : the journal of arthroscopic & related surgery : official publication of the Arthroscopy Association of North America and the International Arthroscopy Association. 2001;17(9):971-80.
8. Lohmander LS, Ostenberg A, Englund M, Roos H. High prevalence of knee osteoarthritis, pain, and functional limitations in female soccer players twelve years after anterior cruciate ligament injury. Arthritis Rheum. 2004;50(10):3145-52.
9. Maletius W, Messner K. Eighteen- to twenty-four-year follow-up after complete rupture of the anterior cruciate ligament. Am J Sports Med. 1999;27(6):711-7.
10. von Porat A, Roos EM, Roos H. High prevalence of osteoarthritis 14 years after an anterior cruciate ligament tear in male soccer players: a study of radiographic and patient relevant outcomes. Ann Rheum Dis. 2004;63(3):269-73.
11. Chaudhari AMW, Briant PL, Bevill SL, Koo S, Andriacchi TP. Knee Kinematics, Cartilage Morphology, and Osteoarthritis after ACL Injury. Medicine & Science in Sports & Exercise. 2008;40(2):215-22.
12. Legnani C, Ventura A, Terzaghi C, Borgo E, Albisetti W. Anterior cruciate ligament reconstruction with synthetic grafts. A review of literature. International Orthopaedics (SICOT). 2010;34(4):465-71.
13. Krudwig WK. Anterior cruciate ligament reconstruction using an alloplastic ligament of polyethylene terephthalate (PET -- Trevira -- hochfest). Follow-up study. Biomed Mater Eng. 2002;12(1):59-67.
14. Lukianov AV, Richmond JC, Barrett GR, Gillquist J. A multicenter study on the results of anterior cruciate ligament reconstruction using a Dacron ligament prosthesis in "salvage" cases. Am J Sports Med. 1989;17(3):380-5; discussion 5-6.
15. Sinagra ZP, Kop A, Pabbruwe M, Parry J, Clark G. Foreign Body Reaction Associated With Artificial LARS Ligaments: A Retrieval Study. Orthop J Sports Med. 2018;6(12):2325967118811604-.

16. Marieswaran M, Jain I, Garg B, Sharma V, Kalyanasundaram D. A Review on Biomechanics of Anterior Cruciate Ligament and Materials for Reconstruction. Applied Bionics and Biomechanics. 2018;2018:4657824.
17. Iliadis DP, Bourlos DN, Mastrokalos DS, Chronopoulos E, Babis GC. LARS Artificial Ligament Versus ABC Purely Polyester Ligament for Anterior Cruciate Ligament Reconstruction. Orthop J Sports Med. 2016;4(6).
18. Daggett M, Redler A, Witte K. Anterior Cruciate Ligament Reconstruction With Suture Tape Augmentation. Arthrosc Tech. 2018;7(4):e385-e9.
19. Evangelopoulos DS, Kohl S, Schwienbacher S, Gantenbein B, Exadaktylos A, Ahmad SS. Collagen application reduces complication rates of mid-substance ACL tears treated with dynamic intraligamentary stabilization. Knee Surg Sports Traumatol Arthrosc. 2017;25(8):2414-9.
20. Robayo LM, Moulin VJ, Tremblay P, Cloutier R, Lamontagne J, Larkin AM, et al. New ligament healing model based on tissue-engineered collagen scaffolds. Wound repair and regeneration : official publication of the Wound Healing Society [and] the European Tissue Repair Society. 2011;19(1):38-48.
21. Nau T, Teuschl A. Regeneration of the anterior cruciate ligament: Current strategies in tissue engineering. World J Orthop. 2015;6(1):127-36.
22. Looney AM, Leider JD, Horn AR, Bodendorfer BM. Bioaugmentation in the surgical treatment of anterior cruciate ligament injuries: A review of current concepts and emerging techniques. SAGE Open Medicine. 2020;8:2050312120921057.
23. Kawakami Y, Nonaka K, Fukase N, Amore AD, Murata Y, Quinn P, et al. A Cell-free Biodegradable Synthetic Artificial Ligament for the Reconstruction of Anterior Cruciate Ligament in a Rat Model. Acta Biomaterialia. 2021;121:275-87.
24. Petrigliano FA, Arom GA, Nazemi AN, Yeranosian MG, Wu BM, McAllister DR. In vivo evaluation of electrospun polycaprolactone graft for anterior cruciate ligament engineering. Tissue engineering Part A. 2015;21(7-8):1228-36.
25. Sensini A, Cristofolini L. Biofabrication of Electrospun Scaffolds for the Regeneration of Tendons and Ligaments. Materials (Basel). 2018;11(10).
26. Moshiri A. Tendon and Ligament Tissue Engineering, Healing and Regenerative Medicine. J Sports Med Doping Stud 2013. 2013;03(02).
27. Mouthuy P-A, Zargar N, Hakimi O, Lostis E, Carr A. Fabrication of continuous electrospun filaments with potential for use as medical fibres. Biofabrication. 2015;7(2):025006.
28. Abhari RE, Mouthuy P-A, Zargar N, Brown C, Carr A. Effect of annealing on the mechanical properties and the degradation of electrospun polydioxanone filaments. Journal of the Mechanical Behavior of Biomedical Materials. 2017;67:127-34.
29. Abhari RE, Carr AJ, Mouthuy P-A. 15 - Multifilament electrospun scaffolds for soft tissue reconstruction. In: Guarino V, Ambrosio L, editors. Electrofluidodynamic Technologies (EFDTs) for Biomaterials and Medical Devices. Woodhead Publishing Series in Biomaterials: Woodhead Publishing; 2018. p. 295-328.
30. Lach AA, Morris HL, Martins JA, Stace ET, Carr AJ, Mouthuy P-A. Pyridine as an additive to improve the deposition of continuous electrospun filaments. PLOS ONE. 2019;14(4):e0214419.
31. Abhari RE, Martins JA, Morris HL, Mouthuy P-A, Carr A. Synthetic sutures: Clinical evaluation and future developments. Journal of Biomaterials Applications. 2017.
32. Abhari RE, Mouthuy PA, Vernet A, Schneider JE, Brown CP, Carr AJ. Using an industrial braiding machine to upscale the production and modulate the design of electrospun medical yarns. Polymer Testing. 2018;69:188-98.
33. Sun H, Mei L, Song C, Cui X, Wang P. The in vivo degradation, absorption and excretion of PCL-based implant. Biomaterials. 2006;27(9):1735-40.

34. Narayanan N, Kuang L, Del Ponte M, Chain C, Deng M. 1 - Design and fabrication of nanocomposites for musculoskeletal tissue regeneration. In: Liu H, editor. Nanocomposites for Musculoskeletal Tissue Regeneration. Oxford: Woodhead Publishing; 2016. p. 3-29.
35. Khan F, Tanaka M, Ahmad SR. Fabrication of polymeric biomaterials: a strategy for tissue engineering and medical devices. J Mater Chem B. 2015;3(42):8224-49.
36. Rueden CT. ImageJ2: ImageJ for the next generation of scientific image data2017 2017.
37. Katta P, Alessandro M, Ramsier RD, Chase GG. Continuous Electrospinning of Aligned Polymer Nanofibers onto a Wire Drum Collector. Nano Lett. 2004;4(11):2215-8.
38. Rueden CT, Schindelin J, Hiner MC, DeZonia BE, Walter AE, Arena ET, et al. ImageJ2: ImageJ for the next generation of scientific image data. BMC bioinformatics. 2017;18(1):529.
39. Murray MM, Flutie BM, Kalish LA, Ecklund K, Fleming BC, Proffen BL, et al. The Bridge-Enhanced Anterior Cruciate Ligament Repair (BEAR) Procedure. Orthop J Sports Med. 2016;4(11).
40. Altman GH, Horan RL, Weitzel P, Richmond JC. The Use of Long-term Bioresorbable Scaffolds for Anterior Cruciate Ligament Repair. JAAOS - Journal of the American Academy of Orthopaedic Surgeons. 2008;16(4):177-87.
41. Silva M, Ferreira FN, Alves NM, Paiva MC. Biodegradable polymer nanocomposites for ligament/tendon tissue engineering. Journal of Nanobiotechnology. 2020;18(1):23.
42. Zhu J, Zhang X, Shao Z, Dai L, Li L, Hu X, et al. In Vivo Study of Ligament-Bone Healing after Anterior Cruciate Ligament Reconstruction Using Autologous Tendons with Mesenchymal Stem Cells Affinity Peptide Conjugated Electrospun Nanofibrous Scaffold. Journal of Nanomaterials. 2013;2013:831873.
43. Bosworth L, Downes S. 1 - Biocompatible three-dimensional scaffolds for tendon tissue engineering using electrospinning. In: Di Silvio L, editor. Cellular Response to Biomaterials: Woodhead Publishing; 2009. p. 3-27.
44. Jiang C, Wang K, Liu Y, Zhang C, Wang B. Textile-based sandwich scaffold using wet electrospun yarns for skin tissue engineering. Journal of the Mechanical Behavior of Biomedical Materials. 2021;119:104499.
45. Bosworth LA. Travelling along the Clinical Roadmap: Developing Electrospun Scaffolds for Tendon Repair. Conference Papers in Science. 2014;2014:304974.
46. Séguéla R. On the Natural Draw Ratio of Semi-Crystalline Polymers: Review of the Mechanical, Physical and Molecular Aspects. Macromol Mater Eng. 2007;292(3):235-44.
47. Latzke PM. Testing and Influencing the Properties of Man-Made Fibers. In: Fourné F, editor. Synthetic Fibers Machines and Equipment, Manufacture, Properties. Munchen, Germany: Hanser Publishers; 1999
48. Uddin NM, Ko F, Xiong J, Farouk B, Capaldi F. Process, Structure, and Properties of Electrospun Carbon Nanotube-Reinforced Nanocomposite Yarns. Research Letters in Materials Science. 2009;2009:868917.
49. Ali U, Zhou Y, Wang X, Lin T. Direct electrospinning of highly twisted, continuous nanofiber yarns. The Journal of The Textile Institute. 2012;103(1):80-8.
50. Zhou Y, Fang J, Wang X, Lin T. Strip twisted electrospun nanofiber yarns: Structural effects on tensile properties. Journal of Materials Research. 2011;27(3):537-44.
51. Joseph J, Nair SV, Menon D. Integrating Substrateless Electrospinning with Textile Technology for Creating Biodegradable Three-Dimensional Structures. Nano Lett. 2015;15(8):5420-6.
52. Yang E, Xu Z, Chur LK, Behroozfar A, Baniasadi M, Moreno S, et al. Nanofibrous Smart Fabrics from Twisted Yarns of Electrospun Piezopolymer. ACS Applied Materials & Interfaces. 2017;9(28):24220-9.

53. Woo SL, Hollis JM, Adams DJ, Lyon RM, Takai S. Tensile properties of the human femur-anterior cruciate ligament-tibia complex. The effects of specimen age and orientation. Am J Sports Med. 1991;19(3):217-25.
54. Pandy MG, Shelburne KB. Dependence of cruciate-ligament loading on muscle forces and external load. Journal of biomechanics. 1997;30(10):1015-24.
55. Hakimi O, Mouthuy PA, Zargar N, Lostis E, Morrey M, Carr A. A layered electrospun and woven surgical scaffold to enhance endogenous tendon repair. Acta Biomater. 2015;26:124-35.
56. Van Dyke RO, Chaudhary SA, Gould G, Trimba R, Laughlin RT. Biomechanical Head-to-Head Comparison of 2 Sutures and the Giftbox Versus Bunnell Techniques for Midsubstance Achilles Tendon Ruptures. Orthop J Sports Med. 2017;5(5):2325967117707477-.
57. Xue J, Wu T, Dai Y, Xia Y. Electrospinning and Electrospun Nanofibers: Methods, Materials, and Applications. Chem Rev. 2019;119(8):5298-415.
58. Qu F, Guilak F, Mauck RL. Cell migration: implications for repair and regeneration in joint disease. Nature reviews Rheumatology. 2019;15(3):167-79.
59. Rashid M, Dudhia J, Dakin SG, Snelling S, Lach A, De Godoy R, et al. Histological evaluation of cellular response to a multifilament electrospun suture for tendon repair. PLOS ONE. 2020;15(6):e0234982.
60. Nezhentsev A, Abhari RE, Baldwin MJ, Mimpen JY, Augustyniak E, Isaacs M, et al. In vitro evaluation of the response of human tendon-derived stromal cells to a novel electrospun suture for tendon repair. Translational Sports Medicine. 2021;4(3):409-18.
61. Horakova J, Klicova M, Erben J, Klapstova A, Novotny V, Behalek L, et al. Impact of Various Sterilization and Disinfection Techniques on Electrospun Poly-ε-caprolactone. ACS Omega. 2020;5(15):8885-92.
62. de Cassan D, Hoheisel AL, Glasmacher B, Menzel H. Impact of sterilization by electron beam, gamma radiation and X-rays on electrospun poly-(ε-caprolactone) fiber mats. J Mater Sci Mater Med. 2019;30(4):42.
63. Bosworth LA, Gibb A, Downes S. Gamma irradiation of electrospun poly(ε-caprolactone) fibers affects material properties but not cell response. Journal of Polymer Science Part B: Polymer Physics. 2012;50(12):870-6.
64. Morris H, Martins J, Lach A, Carr A, Mouthuy PA. Translational path for electrospun and electrosprayed medical devices from bench to bedside. 2021. p. 423-54.